Photoactive Zr and Ti Metal-Organic-Frameworks for solid-state solar cells.

Arianna Melillo,[a] Rocío García-Aboal,[b] Sergio Navalón,[a] Pedro Atienzar,[b] Belén Ferrer,[a] Mercedes Álvaro[a] and Hermenegildo García[b]*

[a] Departamento de Química, Universitat Politècnica de València, Camino de Vera s/n, Valencia 46022, Spain

[b] Instituto Universitario de Tecnología Química, CSIC-UPV, Universitat Politècnica de València, Av. de los Naranjos, Valencia 46022, Spain

E-mail: hgarcia@quim.upv.es

KEYWORDS. Solid-state solar cells; photoactive MOFs

ABSTRACT: Solid-state photovoltaic cells based on robust metal-organic frameworks (MOFs), MIL-125(Ti), MIL-125(Ti)-NH_2, UiO-67, Ru(bpy)$_2$-UiO-67, as active components and spiro-MeOTAD as hole transporting layer have been prepared, observing photovoltaic response that increases with the presence of bathochromic –NH_2 groups on the linker or the presence of Ru (II) polypyridyl complex. These results show that the strategies typically employed in photocatalysis to enhance the photocatalytic activity of MOFs can also be applied in the field of photovoltaic devices.

Introduction

Depletion of fossil fuel reserves and actions to mitigate the climate change caused by the adverse impact on the environment of atmospheric CO_2 emissions have become a decisive driving force for the development of alternative renewable energy sources. Among the various possible primary energy resources, solar energy stands out as an ideal candidate owing to its clean, abundant, and inexhaustible nature. Solar cells, which convert solar into electrical energy based on photo-generated charge separation on a semiconductor, has become a mature technology, the target in this area being the development of affordable materials based on abundant or renewable elements.[1] Therefore, the finding of new semiconductor materials able to harvest the whole sunlight spectrum and exhibiting sufficient stability is highly demanded. Research in this area has grown exponentially in recent years.[2-4] Indeed, long-term stability is one of the main challenges for the third-generation solar cell devices.[2] To improve the power conversion efficiency (PCE) and stability of the third-generation solar cells, the development of nanostructured materials holds a great potential.

MOFs, as a recent category of porous nanomaterials, appear as appealing for this application due to their flexibility in design and preparation.[5, 6] MOFs are crystalline solids whose composition and structure can be easily tuned by combining a large diversity of organic linkers and metal ions/clusters.[7-13] These highly porous materials possess many remarkable characteristics, including extremely high

surface area values, as well as tunable pore volumes and pore size distributions.[8, 9, 12] They have been traditionally employed as porous materials for gas storage,[14, 15] separations,[14, 15] catalysis and photocatalysis,[3, 16-20] optical sensing and even, more recently, for photovoltaic applications.[6] Functionality of organic linkers allows one to introduce response in the solid upon chemical, electrochemical, or photochemical excitation of these units.[3, 6, 21, 22] Since Garcia et all[23] first published the semiconductor behaviour of MOF-5 and its performance as active phase in a photovoltaic cell, some other MOFs containing photoactive ligands or guest molecules have been designed and employed for photovoltaic applications.[1, 24] In some cases, MOF has been used as host of a dye[19, 20] to harvest most of the visible light and/or a suitable electrolyte that matched their energy levels with the valence and conduction band of the MOF is employed for efficient energy conversion. Reports in which only the MOF is used as active phase for the construction of solid-state photovoltaic devices are few and far between. Garcia[25] published the use of commercial MIL-53 (Al_2BDC_3), pristine and as host of electron donor molecules, as active phase for photovoltaic devices. In this work, it was concluded that the efficiency of the photovoltaic device increases with the incorporation of an organic guest. Recently, Shrestha et al[1] have employed an intrinsically p-type conductive Co-based MOFs, formed by coordination of Co (II) ions with di(3-diaminopropyl)-viologen dibromide (DAPV), to build a p-n type heterojunction with thin mesoporous TiO_2 film that was used as active material in a solid-state solar cell, measuring one of the highest efficiency for this type of solid-state devices.

The common limiting factor of the published examples for possible future application in solar cells is the low MOF stability, undergoing performance decay upon operation. A more robust MOF, the UiO-66-NH_2, has recently been used [22] to build a solid state solar cell, without using a TiO_2 mesoporous layer. Incorporation of Ti at the metallic cluster of the MOF increased the current density generated by the device.

Continuing with this research line, and in order to build a MOF sensitized solid state solar cell with long-term stability, it is reported herein the photovoltaic activity of two of the most stable known MOFs whose behavior as semiconductor and photocatalyst has been widely reported, namely, MIL-125(Ti) and UiO-67(Zr).[26, 27] In the present study, these two MOFs have been evaluated as active phase for the construction of solid-state solar cells, without TiO_2 mesoporous layer and using a conductive polymer as hole transporting layer. Since none of these parent MOFs absorbs visible light,[28, 29] the materials that have been tested as active phase in the construction of MOF sensitized solid-state solar cells in the present study are the amino functionalized MIL-125(Ti), having an absorption band at 420 nm, and the UiO-67(Zr) having ruthenium(II)-polypyridyl complexes appended at satellite positions of the backbone.[3, 4, 28, 30]

Experimental procedure

All chemicals were purchased from Sigma-Aldrich and used without further purification.

MIL-125(Ti) synthesis:

MIL-125(Ti) was prepared following the procedure described by Se-NaKim.[31] Briefly, a mixture of *N,N*-dimethylformamide (DMF) and methanol (9:1; 50 mL) was introduced in a Duran bottle of 150 mL. Then, titanium isopropoxide (9 mmol) and 1,4-benzene dicarboxylic acid (15 mmol) were added and the system was sonicated for 30 min. After this time, the mixture was heated in an oven at 150 °C for 16 h. Then, the system was cooled to room temperature. The resulting white powder was filtered and washed twice with DMF and methanol. The final material was dried overnight at 150 °C under vacuum.

MIL-125(Ti)-NH_2 synthesis:

MIL-125(Ti)-NH_2 was prepared following a previously reported procedure.[31] A suspension of 2-aminoterephthalic acid (1.43 g, 7.9 mmol) in 20 mL of anhydrous DMF was introduced in a 30 mL vial.

Then, anhydrous methanol (5 mL) was added to the flask and the system was sonicated for 20 min. The mixture was transferred to a 50 mL Teflon-lined autoclave and titanium isopropoxide (1.36 g, 4.8 mmol) was added. The autoclave was sealed and heated up to 110 °C for 72 h. After cooling to room temperature, the suspension was filtered and washed by suspending the powder in DMF for 12 h. Subsequently, the solid was washed with additional DMF at 120 °C for 12 h. This washing procedure was repeated using methanol as solvent to remove the DMF. The material was collected by filtration and dried overnight in an oven at 100 °C.

Preparation of Ru(II) Bis(2,2′-bipyridine)(2,2′-bipyridyl-5,5′-dicarboxylic acid) dichloride, Rudcbp

Ru(II) bis(2,2′-bipyridine) dichloride, $Ru(bpy)_2Cl_2$, was synthesized according to the procedure described by Sullivan et al.[32] $Ru(bpy)_2Cl_2$ (0.160 g, 0.33 mmol) and 2,2′- bipyridyl-5,5′-dicarboxylic acid (dcbpy, 0.101 g, 0.42 mmol) were introduced in a 500 mL flask and suspended in a 20 mL mixture of EtOH-water and heated overnight at reflux under N_2. The solvent was then removed under reduced pressure and the product was crystallized from MeOH using diethyl ether.

UiO-67(Zr) and Rudcbpy-UiO-67(Zr) synthesis:

A solution of ZrCl4 (0.130 mg, 0.56 mmol) and benzoic acid (3.4 g, 28 mmol) in DMF (20 mL) was introduced in a scintillation vial.[28, 33] The solution was sonicated for several minutes and, then, 140 mg of biphenyl dicarboxylic acid, (BPDC, 0.58 mmol), and 50 mg of Rudcbpy in the case of Rudcbpy-UiO-67(Zr)-doped MOF, were added. The mixture was sonicated for 10 min. The vial was then heated at 120 °C for 48 h. The obtained precipitate was separated by centrifugation and washed 3 times with DMF and 3 times with ethanol. The crystalline solid was characterized by ICP, TGA, BET and PXRD.

Characterization techniques: Powder X-ray diffraction (PXRD) patterns were recorded on a Philips XPert diffractometer equipped with a graphite monochromator (40 kV and 45 mA) employing Ni filtered CuKα radiation. N_2 adsorption isotherms at 77 K were measured using a Micromeritics ASAP 2010 apparatus. Thermogravimetric analyses were performed on a TGA/SDTA851e METTLER TOLEDO station. Diffuse reflectance UV−visible spectra were recorded using a Cary 5000 Varian spectrophotometer having an integrating sphere and using $BaSO_4$ as reference; the sample as compressed powder was placed on a sample holder. The morphology and composition attributed to each MOF were characterized using a SEM instrument (Zeiss instrument, AURIGA Compact) coupled with an EDX detector. ATR-FTIR spectra were measured with a Bruker Tensor 27 instrument. Prior to ATR-FTIR measurements the solid samples were dried in an oven at 100 °C for 16 h to remove physiosorbed water.

***Solid state solar cell preparation*:** All samples were prepared on pre-patterned ITO substrates of 20 mm × 15 mm size with pixel dimensions of 4.5 mm^2 area from Ossila Ltd. ITO substrates were first cleaned by ultrasonic agitation in acetone and isopropanol. The cleaned substrate was then covered with a dense TiO_2 layer of about 20-nm thickness using spin coating. Then, a porous layer of the corresponding MOF sample (thickness 6 μm) was deposited spreading a paste prepared previously by suspending the corresponding MOF sample and terpineol (100 $mg \times mL^{-1}$). The layer was thermally treated in vacuum at 100 °C for 8 h in order to completely remove terpineol. Then, a layer of Spiro-OMeTAD (Merck, 135 mg/mL) in chlorobenzene (containing 38 mM $Li(CF_3SO_2)_2N$, Sigma-Aldrich, and 28 mM 4-tert-butylpyridine) was infiltrated by spin coating at room temperature and left for 1 min, before being spin coated at 2000 rpm for 45 s under nitrogen atmosphere. After spin coating, the film was dried overnight at room temperature in the evaporation chamber. Finally, a gold layer was deposited by thermal evaporation (100 nm). The thickness of the total layers was measured by a MicroXAM-100 3D surface profilometer.

Photovoltaic Response Measurements. To determine the J−V plots, the cell was connected to a sourcemeter (Keithley 2601). The voltage scan was controlled using ReRa Tracer software. The data were automatically transferred to a PC that controlled the experiment and at the same time provided data storage capability to the system. The solar simulator (Sun 2000, ABET Technologies) was equipped with an AM 1.5G filter, and the nominal power for the measurements was 100 mW/cm^2.

The same cells were used to record the photocurrent spectra. In these measurements, the cell was illuminated with a 150 W xenon lamp through a Czerny−Turner monochromator. The current output at short circuit was measured by a potentiostat (AMEL), which transferred the data through the A/D converter card to the PC controlling the monochromator apparatus. Photocurrent curves were corrected using a Newport (818-UV-L) calibrated photodiode.

Results and discussion

The two MOFs under study, namely MIL-125-(Ti)-NH_2 and Rudcbpy-UiO-67(Zr), were synthesized following procedures previously reported in literature.[26, 28, 33] The success of the synthesis was ascertained by X-ray diffraction, thermogravimetry analysis, surface area (BET) measurements and infrared spectroscopy, which showed that the results obtained are in agreement with what was previously reported for these two MOFs. The diffractograms corresponding to the MIL-125(Ti) and MIL-125(Ti)-NH_2 MOFs as well as the pair of diffractograms attributed to the UiO-67(Zr) MOFs show that the parent and substituted materials are isostructural crystalline solids. In fact, the patterns shown in **Figure 1** do not present significant differences in the positions of the peaks for the parent and the derivative MOFs.

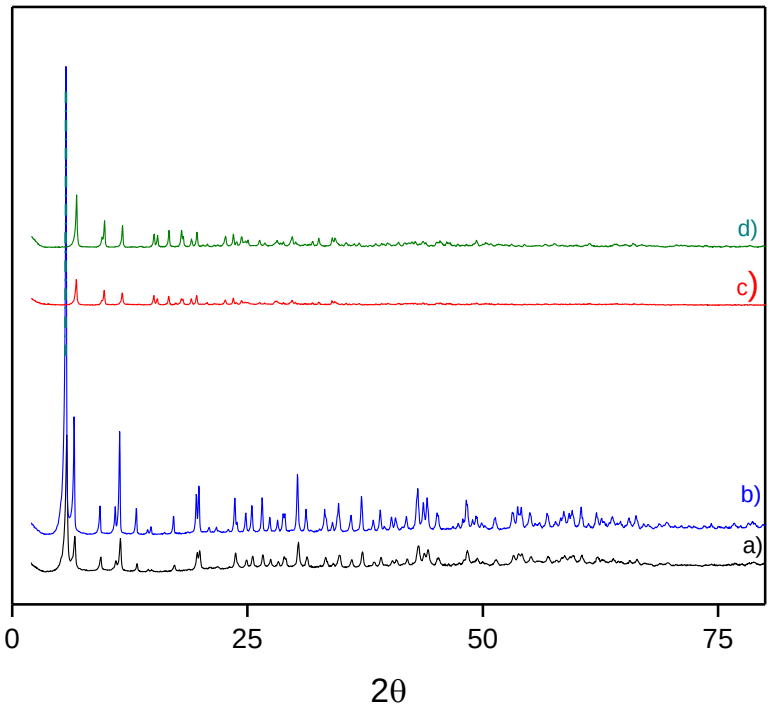

Figure 1. Powder XRD patterns of: a) UiO-67(Zr) and b) Rudcbpy-UiO-67 c) MIL-125(Ti) and d) MIL-125(Ti)-NH_2.

Thermal stability of the MOFs under study was analyzed by thermogravimetry, comparing the parent and derivative MOF. The results are presented in **Figure 2**. These measurements show that MIL-125(Ti) is thermally stable, the first weight loss being observed at 470 °C. In comparison, the MIL-125(Ti)-NH_2 derivative was less stable and started to decompose at 300 °C. In the case of MOF UiO-67(Zr), the solid

exhibits thermal stability up to a temperature of 470 °C, and the incorporation of the Ru complex in Rudcbpy-UiO-67(Zr) MOF determines again somewhat lower stability, observing the first weight loss at a temperature of 400 °C. In any case, the thermogravimetric data show the notable stability of the porous derivative MOFs under study.

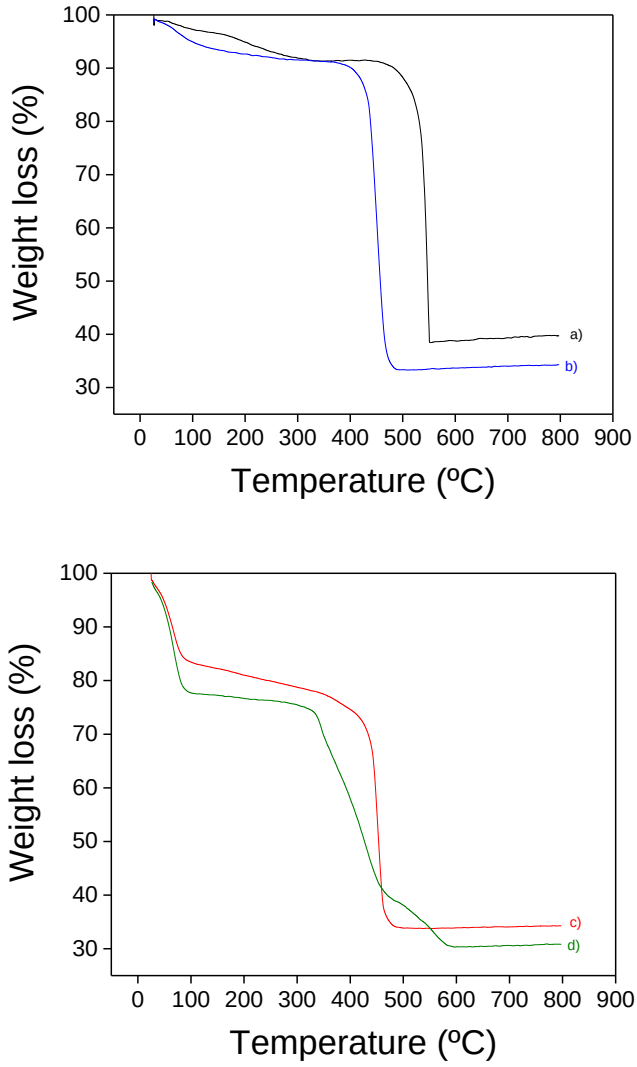

Figure 2. Thermogravimetric analysis of UiO-67 (a), Rudcbpy-UiO-67 (b), MIL-125(Ti) (c) and MIL-125(Ti)-NH_2 (d) MOFs.

The optical spectrum of MIL-125(Ti) reveals that this material absorbs light in the UV region; the presence of $–NH_2$ substituent in MIL-125(Ti)-NH_2 expands its absorption towards the visible by introducing a new electronic transition. A comparison between the two UV-Vis absorption spectra of MIL-125(Ti) is presented in **Figure 3**. The intense band in the UV region with a maximum of 280 nm present in both MIL-125(Ti) and MIL-125(Ti)-NH_2 is associated to the Ti-O ligand to metal charge transfer electronic transition. In the case of the MIL-125(Ti)-NH_2, another absorption band with maximum around 380 nm is recorded due to the electronic transition of the lone electron pair on the N atom to the □* orbital of the aromatic ring.

Comparison of the diffuse reflectance absorption spectra of UiO-67 and Rudcbpy-UiO-67(Zr) MOFs (**Figure 3**) shows the

presence of the absorption band at 460 nm attributable to the Ru polypyridyl complex attached to the crystalline structure. The other band presents in both spectra, at about 275 nm, corresponds to the absorption centered on the biphenyldicarboxylic ligand.

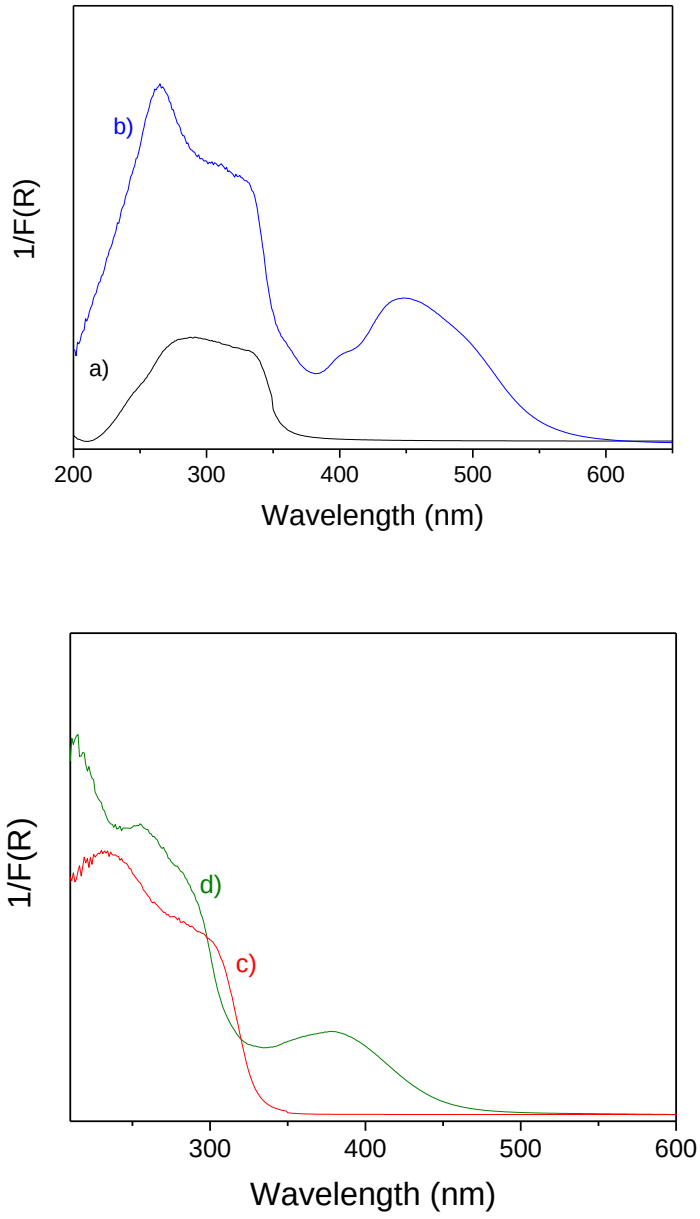

Figure 3. Diffuse reflectance spectra of UiO-67 (a), Rudcbpy-UiO-67 (b), MIL-125(Ti) (c) and MIL-125(Ti)-NH_2 (d) MOFs.

The presence of the NH_2 substituent on the aromatic ring is reflected in the observation in the infrared (IR) spectrum of MIL-125(Ti)-NH_2 of the characteristic vibration bands at 3300, 1610 and 760 cm^{-1} due to N-H vibration and 1255 cm^{-1} for the C-N bond arising from the NH_2 substituent. These characteristic infrared peaks do not appear in the MIL-125(Ti) sample. IR spectrum recorded for the Rudcbpy-UiO-67(Zr) MOF is presented in **Figure 4.** The vibration band at 1409 cm^{-1} is attributed to the asymmetric stretching of carboxylate functional group. The typical vibrations of the aromatic ring are also recorded at 1373 cm^{-1}.

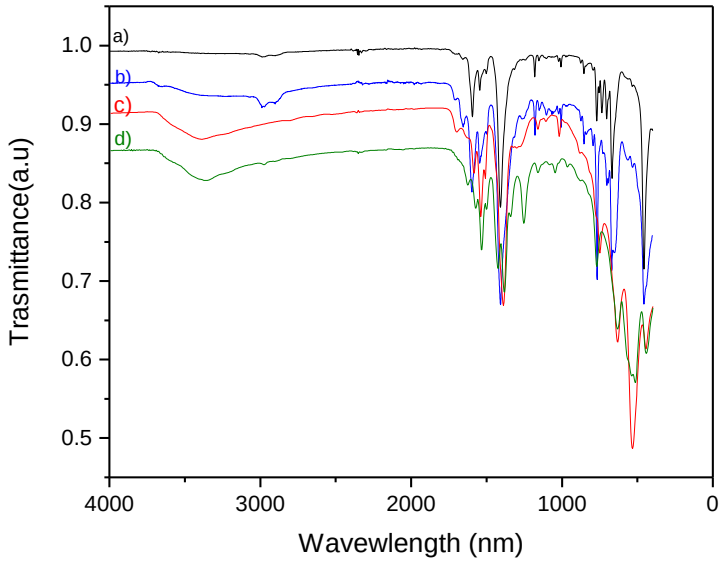

Figure 4. FT-IR spectra of UiO67-Zr (a), Rudcbpy-UiO-67 (b), MIL-125-Ti (c) and MIL-125-Ti-NH_2 (d) MOFs.

It is interesting to note that the materials under study present a very large surface area, as it has been reported in previous works. **Table 1** summarizes the porosity values determined from isothermal gas adsorption for our samples. Specifically, for MIL-125(Ti) MOFs the presence of -NH_2 substituent does not substantially alter the specific surface area of this MOF. In contrast, in the case of UiO-67(Zr) MOFs there is an increase of the surface area from UiO-67(Zr) to Rudcbpy-UiO-67(Zr).

Table 1. BET surface area values of the series of MOFs employed in this work.

MOF	**BET m^2/g**
MIL-125(Ti)	1253
MIL-125(Ti)-NH_2	1200
UiO-67(Zr)	1368
RuBipy-UiO-67(Zr)	1783

Photovoltaic response

To determine the photoactivity of the MOF derivatives of MIL-125(Ti) and UiO-67(Zr) with NH_2 and Rudcbpy, respectively, and considering the long-lived (millisecond time scale) charge separated states previously observed by photophysical studies,[26, 28, 33] a series of photovoltaic devices using the four MOFs, namely, MIL-125, MIL-125-NH_2, UiO-67 and Rudcbpy-UiO-67 as photoactive material, was prepared. Efficient dye sensitized solar cells (DSSCs) typically use a liquid electrolyte to regenerate the neutrality of the dye anchored to the TiO_2 mesoporous structure after electron injection into the

semiconductor conduction band. Although, as commented earlier, there are some precedents in the literature using MOFs in DSSCs, such as the case of Rudcbpy-UiO-67[30] or MOF-5,[34] the use of liquid electrolyte presents drawbacks associated with leakage of the electrolyte or low device stability.

An appropriate alternative is the use of a solid electrolyte or hole transporter material, for this reason, complete solid-state photovoltaic solar cells were prepared. At the present, the only examples of this configuration are the use of Co-DAPV[1] acting as sensitizer and as hole transporter over a mesoporous TiO_2 layer and also the work reported by us using only $Al_2(BDC)_3$.[25] In the last precedent, the only material responsible for the photocurrent was the MOF, since mesoporous TiO_2 scaffold layer was absent.

In the present study, the configuration used in the photovoltaic cell was ITO/TiO_2/MOF/Spiro/Au, where a thin hole blocking layer was deposited between the transparent conducting electrode (ITO) and the MOF material and a transparent hole transport layer of Spiro-MeOTAD is deposited on top of the MOF. **Scheme 1** illustrates the configuration of the devices tested. Finally, a gold metallic layer was deposited on top of a polymer substrate as cathode electrode (see experimental section in the supporting information for the preparation procedure).

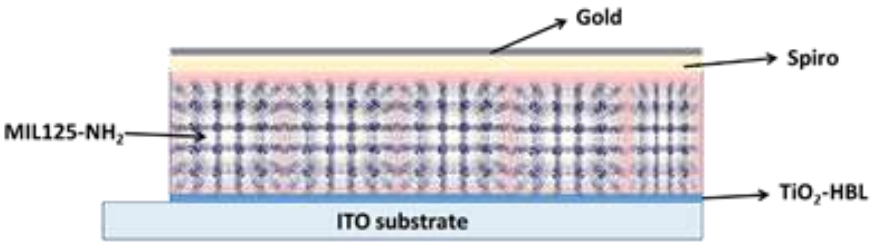

Scheme 1. Device configuration for MOF solar cells of the present study. HBL corresponds to the hole blocking layer.

The morphological features of the MOFs layers incorporated in the devices were studied by FESEM. **Figure 5** shows some representative images. We can see in this Figure 5 for both MOF series, a uniform and porous films constituted by MOF particles with the characteristic spherical shape for MIL-125(Ti) and octahedral geometry in the case of UiO-67(Zr). The thickness of the MOF layers was determined by optical profilometry, measuring 12 ± 2 µm for all samples.

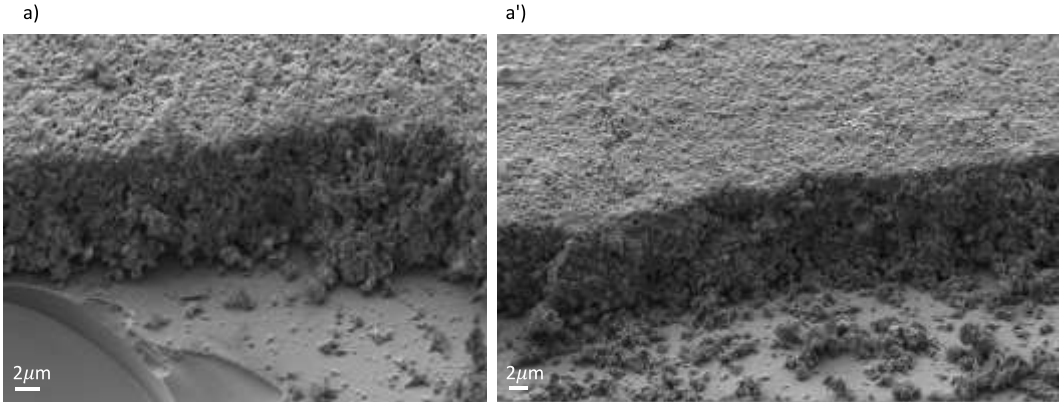

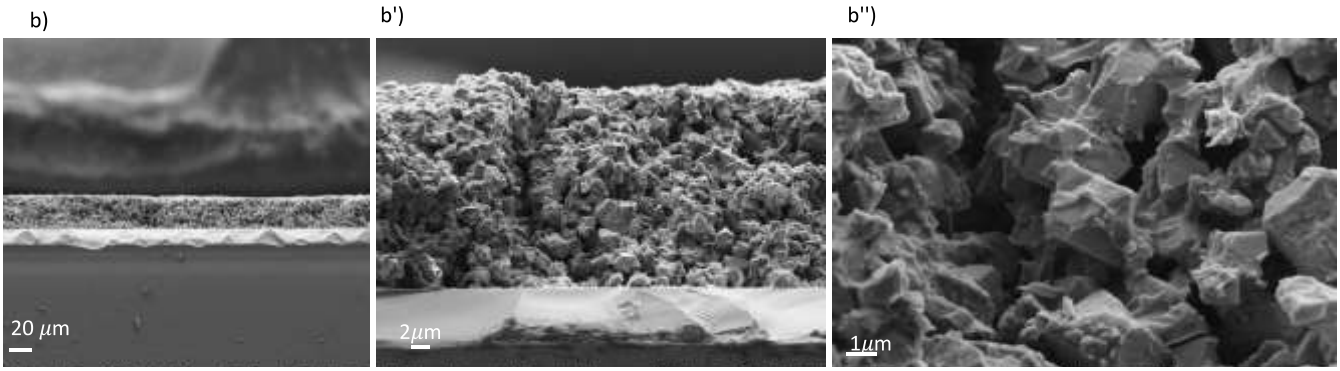

Figure 5. Cross-section SEM images for the devices prepared with MIL-125(Ti)- NH_2 (a and a') and Rubipy-UiO-67(Zr) (b, b' and b'').

Photovoltaic solar cells were characterized with a solar simulator adapted with the AM 1.5G filter and using a nominal power of 100 mW/cm^2 equivalent to one Sun. The performance of these cells is summarized in **Table 2**, while **Figure 6** shows two representative photographs of the solar cells based on MOFs. We were able to observe photovoltaic activity in all the materials studied, MIL-125(Ti)-NH_2 exhibiting the highest current density in the series. The better performance of MIL-125(Ti)-NH_2 can be attributed to a combination of factors, including the long-lived lifetime of the charge separated state and more efficient photoinduced charge separation as previously reported based on transient absorption spectroscopy studies.[35] Also notable is that UiO-67(Zr) containing Rudcbpy dye exhibits an increment of about 40% in the Jsc with respect to the parent UiO-67(Zr). This can be explained considering the visible light photoresponse introduced by the presence of Rudcbpy dye. Previous fundamental photophysical studies by transient absorption spectroscopy has shown that selective photoexcitation of Rudcbpy leads to an initial charge separation at the metal complex, followed by relocation of the charge carriers through the MOF. Also, the voltage at open circuit condition (Voc) exhibits some increase from 381 to 413 mV, a fact that can be attributed to a modification of the quasi-Fermi level of the UiO-67(Zr) associated to the influence of the Rudcbpy dye on the electronic states.

Figure 6. Photograph of the solid-state MIL-125(Ti) (left) and MIL-125(Ti)-NH_2 (right) based solar cells.

Table 2. Photovoltaic performance of solar cells based on the four MOFs under evaluation.

Devices*	Jsc (μA/cm^2)	Voc (mV)	FF (%)
MIL-125(Ti)	12.8	441	27

MIL-125(Ti)-NH_2	24	367	27
UiO-67(Zr)	13.5	381	31
Rudcbpy-UiO-67(Zr)	19	413	45

***Measured under solar simulator (ABET Technologies) equipped with an AM 1.5G filter, and the nominal power for the measurements was 100 mW/cm^2 and the temperature was 25°C.**

In order to correlate the photovoltaic activity with the spectral irradiance, we also measured the photocurrent spectrum of the samples of MIL-125(Ti), MIL-125(Ti)-NH_2, UiO-67(Zr) and Rudcbpy-UiO-67(Zr). **Figure 7** shows the photocurrent of the devices prepared with the MIL-125(Ti) and MIL-125(Ti)-NH_2. Although both materials showed response in the visible region, MIL-125(Ti)-NH_2 exhibits a red-shift respect to the MIL-125(Ti). This red shift agrees with the influence of the –NH_2 substituent on the absorption spectrum of terephthalate MOFs, corresponding to changes in the energy bandgap.[36] On the other hand, the influence of Rudcbpy dye on UiO-67(Zr) derivative is reflected on a new photocurrent band centered at 450 nm which is attributed to the ruthenium complex dye, confirming its role as sensitizer of UiO-67(Zr) MOF. Therefore, although the efficiency values of solid-sate solar cells based on MOFs are still limited, these results demonstrate that strategies generally used in the field of MOFs, such as functionalization with new ligands or the incorporation of organic dyes that expand the photoresponse in the visible spectrum, are also valid to enhance the photovoltaic response of these porous material.

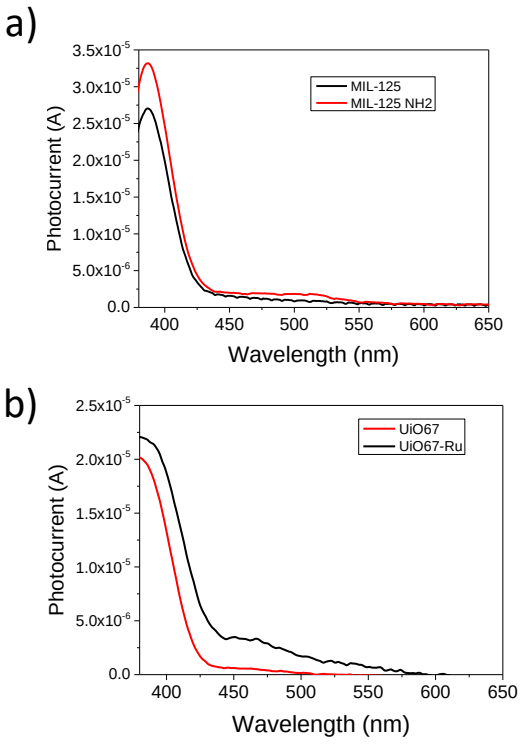

Figure 7. Photocurrent spectra measured for solar cells prepared with: a) MIL-125(Ti) and MIL-125(Ti)-NH_2 and b) UiO-67(Zr) and Rudcbpy-UiO-67(Zr).

Conclusions

The present study has shown the possibility to construct solid-state solar cells based on MOFs, avoiding the use of liquid electrolytes that can deteriorate the crystal structure of MOFs. In addition, it has been shown that general strategies to modify the semiconducting properties of MOF structures are also valid to enhance their photovoltaic response. Thus, functionalization of MIL-125(Ti) with NH_2 groups increases the photovoltaic activity of the parent material due to the higher absorption in the visible region. In addition, functionalization with Rudcbpy dyes acting as sensitizer for the UiO-67 structure also results in an enhancement of the photovoltaic response as consequence of the more efficient light harvesting. It has also been observed that complete solid-state solar cells show a broadening in the photoresponse in the visible region, enhancing the extracted current and device efficiency. The photovoltaic response is in agreement with previous photophysical studies. However, although the results are promising, it is clear that further optimization of, both MOF structure design, particle size, film deposition and cell engineering is necessary to increase the photovoltaic response two orders of magnitude to bring these materials close to real commercial impact. Further work in this direction is currently being carried out.

ACKNOWLEDGMENT

Financial support by the Spanish Ministry of Science and Innovation (Severo Ochoa and RTI2018-98763-CO2-1) and Generalitat Valenciana (Prometeo 2017/083) is gratefully acknowledged.

REFERENCES:

1. Ahn, D. Y.; Lee, D. Y.; Shin, C. Y.; Bui, H. T.; Shrestha, N. K.; Giebeler, L.; Noh, Y.-Y.; Han, S.-H., Novel Solid-State Solar Cell Based on Hole-Conducting MOF-Sensitizer Demonstrating Power Conversion Efficiency of 2.1%. *ACS Applied Materials & Interfaces* **2017,** *9* (15), 12930-12935.
2. García, H.; Navalón, S., *Metal-Organic Frameworks: Applications in Separations and Catalysis*. Wiley: 2018.
3. Dhakshinamoorthy, A.; Asiri, A. M.; García, H., Metal–Organic Framework (MOF) Compounds: Photocatalysts for Redox Reactions and Solar Fuel Production. *Angewandte Chemie International Edition* **2016,** *55* (18), 5414-5445.
4. Wang, J.-L.; Wang, C.; Lin, W., Metal–Organic Frameworks for Light Harvesting and Photocatalysis. *ACS Catalysis* **2012,** *2* (12), 2630-2640.
5. Alvaro, M.; Carbonell, E.; Ferrer, B.; Llabrés i Xamena, F. X.; Garcia, H., Semiconductor Behavior of a Metal-Organic Framework (MOF). *Chemistry A European Journal* **2007,** *13* (18), 5106-5112.
6. Llabrés i Xamena, F. X.; Corma, A.; Garcia, H., Applications for Metal−Organic Frameworks (MOFs) as Quantum Dot Semiconductors. *The Journal of Physical Chemistry C* **2007,** *111* (1), 80-85.
7. Li, H.; Eddaoudi, M.; O'Keeffe, M.; Yaghi, O. M., Design and synthesis of an exceptionally stable and highly porous metal-organic framework. *Nature* **1999,** *402* (6759), 276-279.
8. Férey, G.; Mellot-Draznieks, C.; Serre, C.; Millange, F.; Dutour, J.; Surblé, S.; Margiolaki, I., A Chromium Terephthalate-Based Solid with Unusually Large Pore Volumes and Surface Area. *Science* **2005,** *309* (5743), 2040-2042.
9. Furukawa, H.; Cordova, K. E.; O'Keeffe, M.; Yaghi, O. M., The Chemistry and Applications of Metal-Organic Frameworks. *Science* **2013,** *341* (6149), 1230444.
10. Devic, T.; Serre, C., High valence 3p and transition metal based MOFs. *Chemical Society Reviews* **2014,** *43* (16), 6097-6115.
11. Kitagawa, S.; Kitaura, R.; Noro, S.-i., Functional Porous Coordination Polymers. *Angewandte Chemie International Edition* **2004,** *43* (18), 2334-2375.
12. Yaghi, O. M.; O'Keeffe, M.; Ockwig, N. W.; Chae, H. K.; Eddaoudi, M.; Kim, J., Reticular synthesis and the design of new materials. *Nature* **2003,** *423* (6941), 705-714.
13. Zhou, H.-C.; Long, J. R.; Yaghi, O. M., Introduction to Metal–Organic Frameworks. *Chemical Reviews* **2012,** *112* (2), 673-674.

14. Li, J.-R.; Sculley, J.; Zhou, H.-C., Metal–Organic Frameworks for Separations. *Chemical Reviews* **2012,** *112* (2), 869-932.
15. Zhu, L.; Liu, X.-Q.; Jiang, H.-L.; Sun, L.-B., Metal–Organic Frameworks for Heterogeneous Basic Catalysis. *Chemical Reviews* **2017,** *117* (12), 8129-8176.
16. Li, R.; Zhang, W.; Zhou, K., Metal–Organic-Framework-Based Catalysts for Photoreduction of CO2. *Advanced Materials* **2018,** *30* (35), 1705512.
17. Wang, S.; Wang, X., Multifunctional Metal–Organic Frameworks for Photocatalysis. *Small* **2015,** *11* (26), 3097-3112.
18. Santaclara, J. G.; Kapteijn, F.; Gascon, J.; van der Veen, M. A., Understanding metal–organic frameworks for photocatalytic solar fuel production. *CrystEngComm* **2017,** *19* (29), 4118-4125.
19. Qiu, J.; Zhang, X.; Feng, Y.; Zhang, X.; Wang, H.; Yao, J., Modified metal-organic frameworks as photocatalysts. *Applied Catalysis B: Environmental* **2018,** *231*, 317-342.
20. Khodadadian, F.; Nasalevich, M.; Kapteijn, F.; Stankiewicz, A. I.; Lakerveld, R.; Gascon, J., CHAPTER 8 Photocatalysis: Past Achievements and Future Trends. In *Alternative Energy Sources for Green Chemistry*, The Royal Society of Chemistry: 2016; pp 227-269.
21. Nasalevich, M. A.; Hendon, C. H.; Santaclara, J. G.; Svane, K.; van der Linden, B.; Veber, S. L.; Fedin, M. V.; Houtepen, A. J.; van der Veen, M. A.; Kapteijn, F.; Walsh, A.; Gascon, J., Electronic origins of photocatalytic activity in d0 metal organic frameworks. *Scientific Reports* **2016,** *6* (1), 23676.
22. Santiago Portillo, A.; Baldoví, H. G.; García Fernandez, M. T.; Navalón, S.; Atienzar, P.; Ferrer, B.; Alvaro, M.; Garcia, H.; Li, Z., Ti as Mediator in the Photoinduced Electron Transfer of Mixed-Metal NH2–UiO-66(Zr/Ti): Transient Absorption Spectroscopy Study and Application in Photovoltaic Cell. *The Journal of Physical Chemistry C* **2017,** *121* (12), 7015-7024.
23. Silva, C. G.; Corma, A.; García, H., Metal–organic frameworks as semiconductors. *Journal of Materials Chemistry* **2010,** *20* (16), 3141-3156.
24. Zhu, J.; Maza, W. A.; Morris, A. J., Light-harvesting and energy transfer in ruthenium(II)-polypyridyl doped zirconium(IV) metal-organic frameworks: A look toward solar cell applications. *Journal of Photochemistry and Photobiology A: Chemistry* **2017,** *344*, 64-77.
25. Lopez, H. A.; Dhakshinamoorthy, A.; Ferrer, B.; Atienzar, P.; Alvaro, M.; Garcia, H., Photochemical Response of Commercial MOFs: Al2(BDC)3 and Its Use As Active Material in Photovoltaic Devices. *The Journal of Physical Chemistry C* **2011,** *115* (45), 22200-22206.
26. Dan-Hardi, M.; Serre, C.; Frot, T.; Rozes, L.; Maurin, G.; Sanchez, C.; Férey, G., A New Photoactive Crystalline Highly Porous Titanium(IV) Dicarboxylate. *Journal of the American Chemical Society* **2009,** *131* (31), 10857-10859.
27. Katz, M. J.; Brown, Z. J.; Colón, Y. J.; Siu, P. W.; Scheidt, K. A.; Snurr, R. Q.; Hupp, J. T.; Farha, O. K., A facile synthesis of UiO-66, UiO-67 and their derivatives. *Chemical Communications* **2013,** *49* (82), 9449-9451.
28. Santiago-Portillo, A.; Baldoví, H. G.; Carbonell, E.; Navalón, S.; Álvaro, M.; García, H.; Ferrer, B., Ruthenium(II) Tris(2,2′-bipyridyl) Complex Incorporated in UiO-67 as Photoredox Catalyst. *The Journal of Physical Chemistry C* **2018,** *122* (51), 29190-29199.
29. Nasalevich, M. A.; Goesten, M. G.; Savenije, T. J.; Kapteijn, F.; Gascon, J., Correction: Enhancing optical absorption of metal–organic frameworks for improved visible light photocatalysis. *Chemical Communications* **2015,** *51* (5), 961-962.
30. Maza, W. A.; Haring, A. J.; Ahrenholtz, S. R.; Epley, C. C.; Lin, S. Y.; Morris, A. J., Ruthenium(ii)-polypyridyl zirconium(iv) metal–organic frameworks as a new class of sensitized solar cells. *Chemical Science* **2016,** *7* (1), 719-727.
31. Remiro-Buenamañana, S.; Cabrero-Antonino, M.; Martínez-Guanter, M.; Álvaro, M.; Navalón, S.; García, H., Influence of co-catalysts on the photocatalytic activity of MIL-125(Ti)-NH2 in the overall water splitting. *Applied Catalysis B: Environmental* **2019,** *254*, 677-684.
32. Sullivan, B. P.; Salmon, D. J.; Meyer, T. J., Mixed phosphine 2,2'-bipyridine complexes of ruthenium. *Inorganic Chemistry* **1978,** *17* (12), 3334-3341.

33. Maza, W. A.; Morris, A. J., Photophysical Characterization of a Ruthenium(II) Tris(2,2′-bipyridine)-Doped Zirconium UiO-67 Metal–Organic Framework. *The Journal of Physical Chemistry C* **2014,** *118* (17), 8803-8817.

34. Silva, C. G.; Luz, I.; Llabrés I Xamena, F. X.; Corma, A.; García, H., Water stable Zr-Benzenedicarboxylate metal-organic frameworks as photocatalysts for hydrogen generation. *Chem. Eur. J.* **2010**, 11133-11138.

35. de Miguel, M.; Ragon, F.; Devic, T.; Serre, C.; Horcajada, P.; García, H., Evidence of photoinduced charge separation in the metal-organic framework MIL-125(Ti)-NH2. *Chemphyschem : a European journal of chemical physics and physical chemistry* **2012,** *13* (16), 3651-4.

36. Hendon, C. H.; Tiana, D.; Fontecave, M.; Sanchez, C.; D'arras, L.; Sassoye, C.; Rozes, L.; Mellot-Draznieks, C.; Walsh, A., Engineering the Optical Response of the Titanium-MIL-125 Metal–Organic Framework through Ligand Functionalization. *Journal of the American Chemical Society* **2013,** *135* (30), 10942-10945.

SYNOPSIS TOC